Contribution from the Department of Chemistry,
Columbia University, New York, New York 10027

# Redox Properties of *cis*-Diammineplatinum α-Pyridone Blue and Related Complexes. Synthesis, Structure, and Electrochemical Behavior of *cis*-Diammineplatinum(III) Dimers with Bridging α-Pyridonate Ligands

L. STEVEN HOLLIS and STEPHEN J. LIPPARD*

*Received November 24, 1982*

Orange crystals of the platinum(III) dimer $[(NO_3)(NH_3)_2Pt(C_5H_4NO)_2Pt(NH_3)_2(H_2O)](NO_3)_3 \cdot 2H_2O$ were obtained in 60–80% yield from the chemical oxidation of *cis*-diammineplatinum α-pyridone blue (PPB) with nitric acid. The oxidation process, in which three electrons are removed from the four Pt(2.25) centers of PPB, results in cleavage of the tetranuclear chain to produce a discrete Pt(III) dimer containing a Pt–Pt single bond. The structure of this complex, which contains two bridging α-pyridonate ligands in a head-to-head arrangement, has been determined in a single-crystal X-ray diffraction study (monoclinic unit cell, space group $P2_1/n$, $Z = 4$ with $a = 9.709$ (1) Å, $b = 13.779$ (2) Å, $c = 18.655$ (2) Å, $\beta = 94.44$ (1)°, $V = 2488.2$ Å$^3$). The Pt–Pt distance within the binuclear cation is 2.540 (1) Å with each platinum atom being six-coordinate. The platinum-to-axial-ligand distances of 2.193 (7) Å for $NO_3^-$ and 2.122 (6) Å for $H_2O$ are longer than the normal Pt–O range (1.99–2.07 Å) because of the trans influence of the metal–metal bond. The head-to-tail isomer $[(NO_3)(NH_3)_2Pt(C_5H_4NO)_2Pt(NH_3)_2(NO_3)](NO_3)_2 \cdot {}^1/_2H_2O$ was obtained from nitric acid oxidation of the analogous platinum(II) dimer $[(NH_3)_2Pt(C_5H_4NO)_2Pt(NH_3)_2](NO_3)_2 \cdot 2H_2O$. The structure of this isomer, determined by X-ray crystallographic methods (monoclinic unit cell, space group $C2/c$, $Z = 8$ with $a = 32.447$ (7) Å, $b = 9.404$ (1) Å, $c = 18.199$ (6) Å, $\beta = 123.78$ (2)°; $V = 4615.9$ Å$^3$), is characterized by a Pt–Pt bond distance of 2.547 (1) Å and capping nitrate ligands (Pt–$ONO_2$, 2.170 (10) Å). Cyclic and differential pulse voltammetric studies show that the head-to-tail dimer undergoes a quasi-reversible redox reaction involving a concerted two-electron charge transfer between the $[Pt(II)]_2$ and $[Pt(III)]_2$ forms. These species may also be cleanly interconverted electrochemically as demonstrated by controlled-potential electrolysis studies. The peak potential for the reduction of the platinum(III) dimer is +0.63 V vs. SCE in aqueous 1 M $KNO_3$, pH 1 ($HNO_3$). The head-to-head dimer also displays quasi-reversible two-electron charge-transfer behavior under identical conditions. In this case, however, the charge transfer takes place in two one-electron steps which differ by 50 mV. This result is compatible with the observed formation of PPB during exhaustive electrolytic reduction of the head-to-head platinum(III) dimer.

## Introduction

Study of the reactions of α-pyridone with *cis*-diammine-

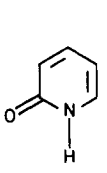

α-pyridone

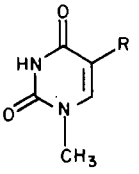

uracil, R = H
thymine, R = $CH_3$

platinum(II) complexes has provided valuable insight into the chemistry of platinum–pyrimidine interactions.[1] The reaction between *cis*-$[Pt(NH_3)_2(H_2O)_2](NO_3)_2$ and α-pyridone produces a variety of mononuclear and binuclear platinum(II) complexes, which have been shown through $^{195}Pt$ NMR and X-ray structural studies[2] to be similar to the products obtained in the analogous reactions with pyrimidines. The advantage of studying the reactivity of the α-pyridone ligand, relative to that of a pyrimidine base such as uracil or thymine, lies in its ability to model these reactions in a simplified fashion by reducing the number of binding sites available to the metal. This feature is particularly effective in clarifying the chemistry of the binuclear and polynuclear platinum complexes produced in these reactions. The chemistry of the polynuclear platinum complexes, which form mixed-valent, metal–metal-bonded species, was not disentangled until the structure of the first crystalline analogue, *cis*-diammineplatinum α-pyridone blue, was determined in 1977.[1]

*cis*-Diammineplatinum α-pyridone blue, $[(NH_3)_2Pt(C_5H_4NO)_2Pt(NH_3)_2]_2(NO_3)_5 \cdot H_2O$ (PPB), is a tetranuclear mixed-valent complex composed of two dimeric *cis*-diammineplatinum units bridged in a head-to-head fashion by α-pyridonate ligands. The two dimeric units are held together through partial metal–metal bonding, which results from the removal of one electron from the tetranuclear chain of platinum $5d_{z^2}$ atomic orbitals.[1c,3] Comparative spectroscopic and chemical studies[1e,f] have shown the platinum–pyrimidine blues[4] to be closely related to the partially oxidized PPB complex. Recently the platinum(II) analogue of PPB and the head-to-head α-pyridonate-bridged platinum(II) dimer have been isolated and structurally characterized (see Figure 1).[2] The head-to-head platinum(II) dimer $[(NH_3)_2Pt(C_5H_4NO)_2Pt(NH_3)_2]_2(NO_3)_4$ has a molecular geometry similar to that of PPB with the exception of longer (0.1–0.2 Å) Pt–Pt distances, which result from differences in metal–metal bond order for the two compounds. The head-to-head platinum(II) complex can be converted, through an overall one-electron oxidation process, to PPB with use of either chemical or electrochemical techniques.[2] The details of this process are of primary importance not only to the study of the platinum–pyrimidine blues but also in understanding the formation of metal–metal bonds in a variety of partially oxidized platinum complexes.

* To whom correspondence should be addressed at the Department of Chemistry, Massachusetts Institute of Technology, Cambridge, MA 02139.

(1) (a) Barton, J. K.; Lippard, S. J. *Ann. N.Y. Acad. Sci.* **1978**, *313*, 686, (b) Barton, J. K.; Lippard, S. J. In "Nucleic Acid-Metal Ion Interactions"; Spiro, T. G., Ed.; Wiley: New York, **1980**; p. 32, (c) Barton, J. K.; Szalda, D. J.; Rabinowitz, H. N.; Waszczak, J. V.; Lippard, S. J. *J. Am. Chem. Soc.* **1979**, *101*, 1434, (d) Barton, J. K.; Rabinowitz, H. N.; Szalda, D. J.; Lippard, S. J. *Ibid.* **1977**, *99*, 2827, (e) Barton, J. K.; Caravana, C.; Lippard, S. J. *Ibid.* **1979**, *101*, 7269, (f) Barton, J. K.; Best, S. A.; Lippard, S. J.; Walton, R. A. *Ibid.* **1978**, *100*, 3785.

(2) (a) Hollis, L. S.; Lippard, S. J. *J. Am. Chem. Soc.* **1981**, *103*, 1230, 6761. (b) Hollis, L. S.; Lippard, S. J. *J. Am. Chem. Soc.* **1983**, *105*, 3494.

(3) Fanwick, P. E.; Hollis, L. S.; Lippard, S. J., to be submitted for publication.

(4) (a) Davidson, J. P.; Faber, P. J.; Fischer, R. G., Jr.; Mansy, S.; Peresie, H. J.; Rosenberg, B.; Van Camp, L. *Cancer Chemother. Rep., Part 1* **1975**, *59*, 287. (b) Lippert, B. *J. Clin. Hematol. Oncol.* **1977**, *7*, 26. (c) Lippert, B.; Pfab, R.; Neugebauer, D. *Inorg. Chim. Acta* **1979**, *37*, L495.

0020-1669/83/1322-2605$01.50/0 

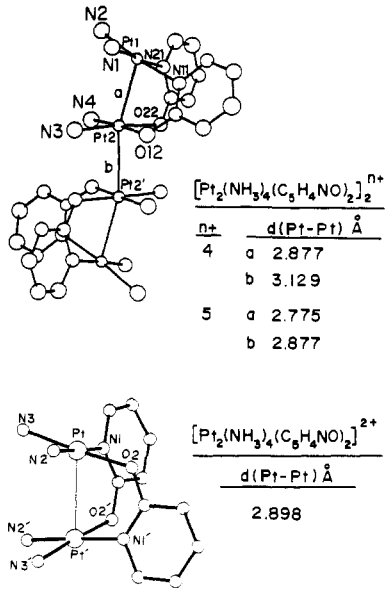


**Figure 1.** Structures of the head-to-head and head-to-tail $\alpha$-pyridonate-bridged dimers of *cis*-diammineplatinum: the head-to-head platinum(II) tetramer $[Pt_2(NH_3)_4(C_5H_4NO)_2]_2^{4+}$ (top, $n = 4$), the mixed-valent tetramer *cis*-diammineplatinum $\alpha$-pyridone blue $[Pt_2(NH_3)_4(C_5H_4NO)_2]_2^{5+}$ (top, $n = 5$), and the head-to-tail platinum(II) dimer $[Pt_2(NH_3)_4(C_5H_4NO)_2]^{2+}$ (bottom).

In this report we examine the redox properties of both head-to-head and head-to-tail $\alpha$-pyridonate-bridged platinum complexes. We show through electrochemical and X-ray structural work that both isomers can be oxidized to discrete dimeric platinum(III) complexes which contain Pt–Pt single bonds. As a follow-up to our preliminary studies,[2,5] we present here the structural details of these compounds and compare the results to the limited structural data presently available on other binuclear platinum(III) complexes. Electrochemical studies on this system, which provide information on the formation of metal–metal bonds both in PPB and in the binuclear Pt(III) complexes, are also presented.

## Experimental Section

**Preparation of Compounds.** Platinum complexes were prepared from *cis*-$[Pt(NH_3)_2Cl_2]$, which was obtained from $K_2PtCl_4$ (Engelhard) by using the method of Dhara.[6] $\alpha$-Pyridone (Aldrich Chemical Co.) was purified by recrystallization from benzene. All other reagents were obtained from commercial sources. Elemental analyses were performed by Galbraith Laboratories, Knoxville, TN.

***cis*-$[(H_2O)(NH_3)_2Pt(C_5H_4NO)_2Pt(NH_3)_2(NO_3)](NO_3)_3\cdot 2H_2O$ (1), Head-to-Head Isomer.** This compound was prepared by oxidizing *cis*-diammineplatinum $\alpha$-pyridone blue (PPB) with nitric acid. The PPB was prepared from the reaction of *cis*-$[Pt(NH_3)_2(H_2O)_2](NO_3)_2$ with $\alpha$-pyridone, as described previously,[1c,2b] and purified by recrystallization from water/0.1 M $HNO_3$. An aqueous solution of PPB (100 mg/20 mL) was warmed on a steam bath with stirring while 5 mL of concentrated nitric acid was added dropwise over a period of 2–3 min. During the addition of nitric acid the solution changed color from blue to red-orange. Air evaporation of the resulting solution provided a 65–80% yield of **1** as red crystals. Anal. Calcd for $Pt_2C_{10}H_{22}N_{10}O_{15}$, the dehydrated form (dried sample) of **1**: C, 13.16; H, 2.43; N, 15.35. Found: C, 13.16; H, 2.45; N, 15.17. UV–visible spectrum of **1** in water: $\lambda$ 254 ($\epsilon \approx 26\,000$ cm$^{-1}$ M$^{-1}$), 268 (sh), 298 (sh), 335 (sh), 408 (sh) nm.

***cis*-$[(NO_3)(NH_3)_2Pt(C_5H_4NO)_2Pt(NH_3)_2(NO_3)](NO_3)_2\cdot{}^1/_2H_2O$ (2), Head-to-Tail Isomer.** The nitrate-capped Pt(III) dimer **2** was prepared by oxidizing the head-to-tail Pt(II) complex, $[(NH_3)_2Pt(C_5H_4NO)_2Pt(NH_3)_2](NO_3)_2\cdot 2H_2O$, with nitric acid, as described above. The head-to-tail platinum(II) dimer was prepared from the reaction that was used to produce PPB[1c,2] and was purified by recrystallization from water. The addition of concentrated nitric acid (5 mL) to the aqueous solution of the platinum(II) complex (100 mg/20 mL) resulted in a clear to red-orange color change. Air evaporation of this solution provided a 70–80% yield of **2** as red crystals. Anal. Calcd for $Pt_2C_{10}H_{20}N_{10}O_{14}$, the dehydrated form (dried sample) of **2**: C, 13.43; H, 2.25; N, 15.66. Found: C, 13.34; H, 2.37; N, 15.56. UV–visible spectrum of **2** in water: $\lambda$ 250 ($\epsilon \approx 21\,000$ cm$^{-1}$ M$^{-1}$), 282 (sh), 302 (sh), 340 (sh), 405 (sh) nm.

Table I. Experimental Details of the X-ray Diffraction Studies of $[Pt_2(NH_3)_4(C_5H_4NO)_2(H_2O)(NO_3)](NO_3)_3\cdot 2H_2O$ (1) and $[Pt_2(NH_3)_4(C_5H_4NO)_2(NO_3)_2](NO_3)_2\cdot{}^1/_2H_2O$ (2)

(A) Crystal Parameters[a] at 23 °C

| | 1 | 2 | | 1 | 2 |
|---|---|---|---|---|---|
| $a$, Å | 9.709 (1) | 32.447 (7) | $Z$ | 4 | 8 |
| $b$, Å | 13.779 (2) | 9.404 (1) | $\rho$(calcd), g cm$^{-3}$ | 2.53 | 2.60 |
| $c$, Å | 18.655 (2) | 18.199 (6) | | | |
| $\beta$, deg | 94.44 (1) | 123.78 (2) | $\rho$(obsd), g cm$^{-3}$ | 2.50 (2)[b] | 2.64 (2)[b] |
| $V$, Å$^3$ | 2488.2 | 4615.9 | | | |
| space group | $P2_1/n$ | $C2/c$ | mol wt | 948.56 | 903.52 |

(B) Measurement of Intensity Data[c]

| | 1 | 2 |
|---|---|---|
| radiation | Mo K$\alpha$ ($\lambda_{\bar{w}} = 0.710\,73$ Å), graphite monochromatized | |
| takeoff angle, deg | 2.0 | 2.0 |
| stds,[d] measd every 1 h of X-ray exposure time | (2,4,6), (2,6,$\bar{4}$), (2,1,$\bar{8}$) | ($\bar{1}$2,4,2), ($\bar{9}$,3,8), (7,5,$\bar{1}$) |
| no. of reflcns collected (excluding systematic absences) | 6354 ($3 < 2\theta < 55°$ ($+h,+k,\pm l$)) | 3815 ($3 < 2\theta < 55°$ ($\pm h,+k,+l$)) |

(C) Treatment of Intensity Data[e]

| | 1 | 2 |
|---|---|---|
| $\mu$, cm$^{-1}$ | 114.4 | 123.4 |
| transmission factor range[f] | 0.19–0.60 | 0.19–0.42 |
| averaging, $R_{av}$[c] | 0.027 | 0.023 |
| no. of reflecns after averaging | 5715 | 3700 |
| obsd unique data ($F_o > n\sigma(F_o)$) | 4148, $n = 4$ | 2634, $n = 2$ |

[a] From a least-squares fit of the setting angles of 25 reflections with $2\theta > 30°$. [b] By suspension in a mixture of $CHBr_3$ and $CHCl_3$. [c] See ref 9 for further details. [d] Showed no decay during data collection. [e] $F_o$ and $\sigma(F_o)$ were corrected for background, attenuator, and Lorentz-polarization of X radiation as described previously.[9] [f] Absorption corrections were performed with the Wehe–Busing–Levy ORABS program.

**Electrochemical Methods.** Cyclic voltammetry (CV) and controlled-potential coulometry (CPC) experiments were performed with a Princeton Applied Research (PAR) Model 173 potentiostat equipped with a Model 179 digital coulometer and a Model 175 universal programer. Differential pulse voltammetry (DPV) was carried out with a PAR Model 174A analyzer. DPV and slow-scan (<500 mV s$^{-1}$) CV data were recorded on a Houston Instruments Model 2000 X-Y recorder. A Tektronix 564 storage oscilloscope was used to record CV data at scan rates exceeding 500 mV s$^{-1}$. All CV and DPV experiments were performed in 1 M $KNO_3$ (adjusted to pH 1 with nitric acid) by using a three-electrode system consisting of a platinum-bead working electrode, a platinum wire loop auxiliary electrode, and a PAR saturated calomel (SCE) reference electrode separated from the working solution by a Vycor plug. Measurements were made at 25 °C under deoxygenated conditions ($N_2$). The electrode performance was monitored by measuring the Fe(II)/Fe(III) couple in an aqueous solution of $K_3Fe(CN)_6$ (5 mg/10 mL in 1 M $KNO_3$). CPC experiments were carried out under identical conditions in a standard H-cell with a platinum-loop working electrode. The test solution was stirred under a stream of nitrogen during the CPC measurement, which was made with background compensation at a potential ~200 mV beyond the peak of interest. Satisfactory coulometric determinations were obtained on aqueous $K_3Fe(CN)_6$ standards. All DPV measurements were made at a sweep rate of 2 mV s$^{-1}$ with a pulse height of 10 mV and a "drop time" of 0.5 s.

**Collection and Reduction of X-ray Data. *cis*-$[Pt_2(NH_3)_4(C_5H_4NO)_2(H_2O)(NO_3)](NO_3)_3\cdot 2H_2O$ (1), Head-to-Head Dimer.** The red crystal chosen for the diffraction study was a parallelepiped with

(5) Hollis, L. S.; Lippard, S. J. *Inorg. Chem.* **1982**, *21*, 2116.
(6) Dhara, S. G. *Indian J. Chem.* **1970**, *8*, 193.

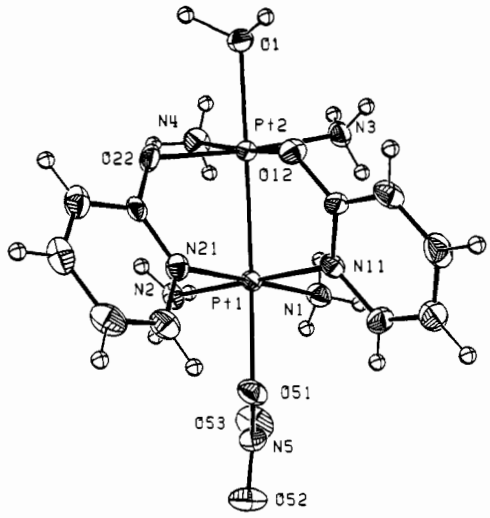


**Figure 2.** ORTEP illustrations of the structure of the head-to-head isomer of the α-pyridonate-bridged cation $[Pt_2(NH_3)_4(C_5H_4NO)_2(H_2O)(NO_3)]^{3+}$ (**1**) showing the 40% probability thermal ellipsoids. For clarity the hydrogen atoms are depicted as spheres with $B$ set to 1 Å$^2$. The labels of the carbon atoms (not shown) are arranged according to their ring number followed by their ring position; for example ring 1 contains N11, C12–C16. The hydrogen atom labels (not shown) are assigned according to the atom to which they are attached (e.g. H1N2 is attached to N2 and H16 to C16).

dimensions of 0.15 mm × 0.15 mm × 0.05 mm and was bounded by the following faces: $(10\bar{1})$, $(\bar{1}01)$, $(01\bar{2})$, $(0\bar{1}2)$, $(0\bar{1}\bar{2})$, (012). The quality of the crystal was examined by taking open-counter ω scans of several low-angle reflections and was found to be acceptable ($\Delta\omega_{1/2} \approx 0.08°$). The unit cell parameters and intensity data were measured with a single-crystal diffractometer as described in Table I. The space group was determined to be $P2_1/n$ ($C_{2h}^5$,No. 14, in a nonstandard setting)[7] from the systematic absences: $h0l$, $h + l = 2n + 1$; $0k0$, $k = 2n + 1$. Further details of the data collection and reduction are presented in Table I.

***cis*-$[Pt_2(NH_3)_4(C_5H_4NO)_2(NO_3)_2](NO_3)_2 \cdot {}^1/_2H_2O$ (2), Head-to-Tail Dimer.** The red crystal used in the diffraction study was a plate with dimensions of 0.06 mm × 0.20 mm × 0.12 mm, bounded by the faces (100), $(\bar{1}00)$, $(\bar{1}11)$, $(1\bar{1}\bar{1})$, $(\bar{1}\bar{1}1)$, and $(01\bar{2})$. Inspection of several low-angle ω scans indicated the crystal to be acceptable for data collection ($\Delta\omega_{1/2} \approx 0.08°$). The space group was determined to be either $C2/c$ ($C_{2h}^6$, No. 15) or $Cc$ ($C_s^4$, No. 9)[8] from the systematic absences, and the former choice was confirmed by the successful solution and refinement of the structure. Further details of the data collection are presented in Table I and ref 9.

**Structure Solution and Refinement. $[Pt_2(NH_3)_4(C_5H_4NO)_2(H_2O)(NO_3)](NO_3)_3 \cdot 2H_2O$ (1).** The structure was solved by Patterson and difference Fourier methods and refined[10] with anisotropic thermal parameters for all non-hydrogen atoms. Neutral-atom scattering factors and anomalous dispersion corrections for all non-hydrogen atoms were obtained from ref 11. Hydrogen atom scattering factors were taken from ref 12. The positions of all C–H and N–H hydrogen atoms were refined with constraints using isotropic thermal parameters. The hydrogen atoms of the pyridonate rings were placed at calculated positions ($d$(C–H) = 0.95 Å) and constrained to "ride" on the carbon atoms to which they are attached.[10] The hydrogen atoms of the ammine ligands were refined as rigid groups by fixing[10] the interatomic distances N–H = 0.87 (1) Å, H–H = 1.42 (1) Å, and Pt–H = 2.50 (1) Å for each hydrogen in the group. The hydrogen atoms of each pyridonate ring and of each ammine ligand (except N6) were given an independent set of common thermal parameters in the refinement. The hydrogen atoms of the ammine ligand N6 were refined with fixed isotropic thermal parameters ($U$ = 0.06 Å$^2$). The positions of the hydrogen atoms attached to water molecules O1 and O3 were located from a difference Fourier map. These hydrogen atoms were included in subsequent cycles of least-squares refinement using fixed positional parameters and an independent set of common thermal parameters of each $H_2O$ molecule. The hydrogen atoms of the water molecule O2 were not located.

Full-matrix least-squares refinement of the structure using 397 parameters converged at $R_1$ = 0.033 and $R_2$ = 0.042.[13] The function

**Table II.** Final Positional Parameters for $[Pt_2(NH_3)_4(C_5H_4NO)_2(H_2O)(NO_3)](NO_3)_3 \cdot 2H_2O$ (1)[a]

| ATOM | X | Y | Z |
|---|---|---|---|
| Pt1 | -0.16528(3) | 0.24873(2) | 0.32289(2) |
| Pt2 | 0.07932(4) | 0.22672(2) | 0.37930(2) |
| O12 | -0.0087(7) | 0.2311(4) | 0.4729(3) |
| N11 | -0.2217(7) | 0.1923(5) | 0.4174(4) |
| C12 | -0.1344(9) | 0.2006(6) | 0.4765(5) |
| C13 | -0.1805(11) | 0.1760(7) | 0.5443(5) |
| H13 | -0.1201(11) | 0.1839(7) | 0.5864(5) |
| C14 | -0.3102(11) | 0.1415(7) | 0.5498(6) |
| H14 | -0.3415(11) | 0.1252(7) | 0.5953(6) |
| C15 | -0.3964(11) | 0.1305(7) | 0.4863(6) |
| H15 | -0.4868(11) | 0.1048(7) | 0.4883(6) |
| C16 | -0.3510(10) | 0.1565(7) | 0.4229(5) |
| H16 | -0.4112(10) | 0.1498(7) | 0.3806(5) |
| O22 | 0.0914(6) | 0.3721(4) | 0.3778(3) |
| N21 | -0.1454(8) | 0.3826(5) | 0.3706(4) |
| C22 | -0.0208(9) | 0.4224(6) | 0.3866(4) |
| C23 | -0.0072(12) | 0.5173(7) | 0.4114(5) |
| H23 | 0.0818(12) | 0.5455(7) | 0.4204(5) |
| C24 | -0.1242(12) | 0.5699(7) | 0.4225(5) |
| H24 | -0.1171(12) | 0.6351(7) | 0.4389(5) |
| C25 | -0.2530(11) | 0.5263(7) | 0.4095(5) |
| H25 | -0.3341(11) | 0.5604(7) | 0.4199(5) |
| C26 | -0.2630(11) | 0.4350(6) | 0.3820(5) |
| H26 | -0.3515(11) | 0.4072(6) | 0.3704(5) |
| N1 | -0.1860(8) | 0.1165(5) | 0.2727(4) |
| N2 | -0.1104(8) | 0.3093(5) | 0.2287(4) |
| N3 | 0.0856(8) | 0.0791(5) | 0.3846(4) |
| N4 | 0.1862(9) | 0.2313(5) | 0.2900(4) |
| N5 | -0.4455(9) | 0.2644(6) | 0.2309(5) |
| O51 | -0.3822(7) | 0.2836(5) | 0.2923(3) |
| O52 | -0.5630(8) | 0.2975(6) | 0.2213(4) |
| O53 | -0.3887(9) | 0.2212(5) | 0.1838(4) |
| O1 | 0.2745(6) | 0.2210(4) | 0.4388(3) |
| N6 | 0.1942(8) | 0.0843(5) | 0.5875(4) |
| O61 | 0.1356(9) | 0.0356(5) | 0.5379(4) |
| O62 | 0.2745(9) | 0.1505(6) | 0.5731(4) |
| O63 | 0.1743(8) | 0.0654(5) | 0.6517(4) |
| N7 | 0.0807(10) | 0.5101(6) | 0.2072(5) |
| O71 | -0.0363(8) | 0.5186(6) | 0.2295(5) |
| O72 | 0.1333(9) | 0.5759(6) | 0.1740(4) |
| O73 | 0.1451(9) | 0.4320(5) | 0.2182(4) |
| N8 | 0.1151(12) | 0.1315(8) | 0.1124(6) |
| O81 | 0.1157(11) | 0.0939(8) | 0.0527(6) |
| O82 | 0.2147(12) | 0.1135(10) | 0.1551(6) |
| O83 | 0.0218(11) | 0.1830(7) | 0.1276(6) |
| O2 | 0.4490(9) | 0.4991(6) | 0.2616(5) |
| O3 | 0.4139(9) | 0.3802(6) | 0.4396(5) |
| H1N1 | -0.247(5) | 0.1198(16) | 0.236(2) |
| H2N1 | -0.214(6) | 0.0724(12) | 0.3021(13) |
| H3N1 | -0.107(2) | 0.098(2) | 0.258(3) |
| H1N2 | -0.181(2) | 0.339(4) | 0.2064(18) |
| H2N2 | -0.082(6) | 0.2646(12) | 0.2000(15) |
| H3N2 | -0.044(5) | 0.351(4) | 0.2372(9) |
| H1N3 | 0.009(4) | 0.0531(9) | 0.365(4) |
| H2N3 | 0.096(8) | 0.0588(9) | 0.4293(7) |
| H3N3 | 0.155(5) | 0.0556(10) | 0.362(4) |
| H1N4 | 0.200(6) | 0.2912(10) | 0.276(2) |
| H2N4 | 0.142(4) | 0.201(4) | 0.2535(11) |
| H3N4 | 0.268(3) | 0.204(4) | 0.2973(14) |
| H101 | 0.3549 | 0.2798 | 0.4257 |
| H201 | 0.2785 | 0.2050 | 0.4820 |
| H103 | 0.4037 | 0.4525 | 0.4401 |
| H203 | 0.4143 | 0.3462 | 0.5008 |

[a] Atoms are labeled as shown in Figure 2. The atoms of the pyridonate rings are labeled according to their ring number followed by their ring position; for example, ring 1 contains N11, C12–C16, etc. Estimated standard deviations in the last significant digit(s) are given in parentheses.


(7) "International Tables for X-ray Crystallography," 3rd ed.; Kynoch Press: Birmingham, England, 1973; Vol. I, p 99.
(8) Reference 7, pp 89, 101.
(9) Silverman, L. D.; Dewan, J. C.; Giandomenico, C. M.; Lippard, S. J. *Inorg. Chem.* **1980**, *19*, 3379.
(10) All calculations were performed on a DEC VAX-11/780 computer using SHELX-76: Sheldrick G. M. In "Computing in Crystallography"; Schenk, H., Olthof-Hazekamp, R., van Koningsveld, H., Bassi, G. C., Eds.; Delft University Press: Delft, The Netherlands, 1978; pp 34–42.
(11) "International Tables for X-ray Crystallography"; Kynoch Press: Birmingham, England, 1974; Vol. IV, pp 99, 149.
(12) Stewart, R. F.; Davidson, E. R.; Simpson, W. T. *J. Chem. Phys.* **1965**, *42*, 3175.

**Table III.** Final Positional Parameters for $[Pt_2(NH_3)_4(C_5H_4NO)_2(NO_3)_2](NO_3)_2 \cdot {}^1/_2H_2O$ (2)[a]

| ATOM | X | Y | Z |
|---|---|---|---|
| Pt1 | 0.61913(2) | 0.11156(6) | 0.25882(3) |
| Pt2 | 0.62223(2) | 0.35619(6) | 0.20203(3) |
| N1 | 0.5821(4) | 0.0090(11) | 0.1395(6) |
| N2 | 0.5544(4) | 0.1318(12) | 0.2518(8) |
| N3 | 0.5603(4) | 0.3446(12) | 0.0748(6) |
| N4 | 0.5826(4) | 0.4614(12) | 0.2427(6) |
| O12 | 0.6829(3) | 0.0790(9) | 0.2677(5) |
| N11 | 0.6639(4) | 0.2576(11) | 0.1661(6) |
| C12 | 0.6902(4) | 0.1440(14) | 0.2114(7) |
| C16 | 0.6718(6) | 0.3136(15) | 0.1060(9) |
| H16 | 0.6521(6) | 0.3923(15) | 0.0716(9) |
| C15 | 0.7059(6) | 0.2641(15) | 0.0929(9) |
| H15 | 0.7099(6) | 0.3062(15) | 0.0498(9) |
| C14 | 0.7350(5) | 0.1514(16) | 0.1428(9) |
| H14 | 0.7606(5) | 0.1177(16) | 0.1368(9) |
| C13 | 0.7267(5) | 0.0884(15) | 0.2014(9) |
| H13 | 0.7454(5) | 0.0077(15) | 0.2347(9) |
| O22 | 0.6826(3) | 0.3812(9) | 0.3234(5) |
| N21 | 0.6565(4) | 0.2084(12) | 0.3780(6) |
| C22 | 0.6822(5) | 0.3252(16) | 0.3903(8) |
| C23 | 0.7100(5) | 0.3916(16) | 0.4734(8) |
| H23 | 0.7286(5) | 0.4753(16) | 0.4823(8) |
| C24 | 0.7095(6) | 0.331(2) | 0.5424(8) |
| H24 | 0.7280(6) | 0.373(2) | 0.5994(8) |
| C25 | 0.6829(7) | 0.2098(18) | 0.5286(10) |
| H25 | 0.6825(7) | 0.1675(18) | 0.5756(10) |
| C26 | 0.6567(5) | 0.1523(15) | 0.4471(8) |
| H26 | 0.6380(5) | 0.0686(15) | 0.4375(8) |
| N6 | 0.6227(6) | 0.6697(17) | 0.1511(9) |
| O61 | 0.6470(4) | 0.5528(11) | 0.1766(6) |
| O62 | 0.5788(5) | 0.6681(12) | 0.1228(8) |
| O63 | 0.6464(6) | 0.7761(14) | 0.1612(9) |
| N5 | 0.6567(5) | -0.1717(19) | 0.3557(8) |
| O51 | 0.6175(4) | -0.1029(11) | 0.3012(6) |
| O52 | 0.6953(4) | -0.1103(12) | 0.4067(7) |
| O53[b] | 0.6531(4) | -0.3009(14) | 0.3549(7) |
| N7 | 0.5486 | 0.5986 | -0.0966 |
| O71 | 0.5240(6) | 0.5442(19) | -0.0726(10) |
| O72 | 0.5889(6) | 0.552(2) | -0.0722(14) |
| O73 | 0.5292(8) | 0.679(2) | -0.1589(16) |
| O74 | 0.5165 | 0.6734 | -0.1013 |
| O75 | 0.5648 | 0.5002 | -0.0445 |
| O76 | 0.5740 | 0.6480 | -0.1204 |
| N8 | 0.0473(6) | 0.4266(18) | 0.4288(8) |
| O81 | 0.0170(5) | 0.4069(17) | 0.4477(9) |
| O82 | 0.0321(6) | 0.451(2) | 0.3507(10) |
| O83 | 0.0882(5) | 0.3958(16) | 0.4843(9) |
| O1 | 0.0000 | 0.156(3) | 0.2500 |
| H1N4 | 0.5511(6) | 0.463(8) | 0.200(2) |
| H2N4 | 0.586(3) | 0.419(5) | 0.288(4) |
| H3N4 | 0.593(2) | 0.549(3) | 0.257(5) |
| H1N3 | 0.5622(15) | 0.271(5) | 0.0477(18) |
| H2N3 | 0.5336(4) | 0.336(9) | 0.0754(11) |
| H3N3 | 0.5576(17) | 0.421(4) | 0.0454(17) |
| H1N2 | 0.5582(10) | 0.186(7) | 0.294(3) |
| H2N2 | 0.5311(9) | 0.170(8) | 0.201(2) |
| H3N2 | 0.5433(16) | 0.0491(20) | 0.256(5) |
| H1N1 | 0.571(3) | 0.069(2) | 0.0959(7) |
| H2N1 | 0.6012(11) | -0.053(6) | 0.137(2) |
| H3N1 | 0.5562(18) | -0.037(7) | 0.131(3) |

[a] Atoms are labeled as shown in Figure 3. Estimated standard deviations in the last significant digit(s) are given in parentheses. [b] Nitrate N7 is disordered over two positions with a site occupation factor of 0.747 for N7, O71, O72, O73 and 0.253 for N7, O74, O75, O76.

minimized during refinement was $\sum w(|F_o| - |F_c|)^2$, where $w = 0.9329/[\sigma^2(F_o) + 0.000625F_o^2]$. The maximum parameter shift/esd in the final cycle of refinement was 0.1 (H1N2 position), and the largest peaks (<2.5 e Å$^{-3}$) on the difference map were in the vicinity of the Pt atoms (≤0.9 Å). The average $w\Delta^2$ for groups of data sectioned according to parity group, $(\sin\theta)/\lambda$, $|F_o|$, $|h|$, $|k|$, or $|l|$, showed good consistency, and the weighting scheme was considered to be acceptable.

The final atomic positional parameters, together with their estimated standard deviations, are reported in Table II. The interatomic distances and angles are contained with their estimated standard deviations in Table IV. A complete listing of atomic positional and thermal parameters for compound **1** (Table S1) and a listing of final observed and calculated structure factors (Table S3) are available as supplementary material. Figure 2 depicts the coordination geometry and atom-labeling scheme for the $[Pt_2(NH_3)_4(C_5H_4NO)_2(H_2O)(NO_3)]^{3+}$ cation.

(13) $R_1 = \sum||F_o| - |F_c||/\sum|F_o|$; $R_2 = [\sum w(|F_o| - |F_c|)^2/\sum w|F_o|^2]^{1/2}$.

**Table IV.** Interatomic Distances (Å) and Angles (deg) for $[Pt_2(NH_3)_4(C_5H_4NO)_2(H_2O)(NO_3)](NO_3)_3 \cdot 2H_2O$ (1)[a]

| | | | |
|---|---|---|---|
| **Coordination Sphere** | | | |
| Pt1-Pt2 | 2.5401(5) | Pt2-N3 | 2.038(6) |
| Pt1-N1 | 2.051(6) | Pt2-N4 | 2.031(7) |
| Pt1-N2 | 2.052(7) | Pt2-O12 | 2.003(6) |
| Pt1-N11 | 2.040(7) | Pt2-O22 | 2.007(5) |
| Pt1-N21 | 2.051(7) | Pt2-O1 | 2.122(6) |
| Pt1-O51 | 2.193(7) | | |
| Pt2-Pt1-O51 | 169.3(2) | Pt1-Pt2-O1 | 171.7(2) |
| N1-Pt1-N2 | 89.6(3) | N3-Pt2-N4 | 93.2(3) |
| N1-Pt1-N11 | 91.9(3) | N3-Pt2-O12 | 90.1(3) |
| N1-Pt1-N21 | 178.6(3) | N3-Pt2-O22 | 174.7(3) |
| N2-Pt1-N11 | 178.4(3) | N4-Pt2-O12 | 173.5(3) |
| N2-Pt1-N21 | 89.1(3) | N4-Pt2-O22 | 85.6(3) |
| N11-Pt1-N21 | 89.4(3) | O12-Pt2-O22 | 90.6(3) |
| O51-Pt1-N1 | 91.0(3) | O1-Pt2-N3 | 85.1(3) |
| O51-Pt1-N2 | 89.8(3) | O1-Pt2-N4 | 86.4(3) |
| O51-Pt1-N11 | 89.5(3) | O1-Pt2-O12 | 88.3(2) |
| O51-Pt1-N21 | 88.4(3) | O1-Pt2-O22 | 89.6(2) |
| **Ligand Geometry** | | | |
| O12-C12 | 1.298(10) | O22-C22 | 1.312(10) |
| N11-C12 | 1.343(10) | N21-C22 | 1.340(11) |
| C12-C13 | 1.414(12) | C22-C23 | 1.390(12) |
| C13-C14 | 1.357(14) | C23-C24 | 1.377(15) |
| C14-C15 | 1.405(14) | C24-C25 | 1.392(15) |
| C15-C16 | 1.343(13) | C25-C26 | 1.359(13) |
| C16-N11 | 1.360(11) | C26-N21 | 1.382(11) |
| O12-N11 | 2.303(9) | O22-N21 | 2.297(10) |
| N5-O51 | 1.284(10) | N5-O53 | 1.227(11) |
| N5-O52 | 1.229(11) | | |
| Pt1-N11-C12 | 118.9(6) | Pt1-N21-C22 | 121.2(6) |
| Pt1-N11-C16 | 121.0(6) | Pt1-N21-C26 | 119.6(7) |
| Pt2-O12-C12 | 120.2(5) | Pt2-O22-C22 | 118.4(5) |
| C12-N11-C16 | 119.7(8) | C22-N21-C26 | 119.6(7) |
| O12-C12-N11 | 121.4(8) | O22-C22-N21 | 120.0(7) |
| O12-C12-C13 | 119.3(8) | O22-C22-C23 | 118.6(8) |
| N11-C12-C13 | 119.4(8) | N21-C22-C23 | 121.3(8) |
| C12-C13-C14 | 120.8(9) | C22-C23-C24 | 119.2(9) |
| C13-C14-C15 | 118.0(9) | C23-C24-C25 | 119.1(9) |
| C14-C15-C16 | 119.9(10) | C24-C25-C26 | 120.2(10) |
| C15-C16-N11 | 122.1(10) | C25-C26-N21 | 120.4(10) |
| Pt1-O51-N5 | 124.8(6) | O51-N5-O53 | 121.9(8) |
| O51-N5-O52 | 115.3(9) | O52-N5-O53 | 122.6(9) |
| **Anion Geometry** | | | |
| N6-O61 | 1.244(9) | O61-N6-O62 | 119.6(8) |
| N6-O62 | 1.243(10) | O61-N6-O63 | 120.1(8) |
| N6-O63 | 1.254(10) | O62-N6-O63 | 120.3(8) |
| N7-O71 | 1.244(11) | O71-N7-O72 | 121.6(9) |
| N7-O72 | 1.231(10) | O71-N7-O73 | 118.9(9) |
| N7-O73 | 1.254(10) | O72-N7-O73 | 119.5(10) |
| N8-O81 | 1.228(13) | O81-N8-O82 | 116.3(13) |
| N8-O82 | 1.229(14) | O81-N8-O83 | 121.3(13) |
| N8-O83 | 1.201(13) | O82-N8-O83 | 122.4(13) |
| **Hydrogen Atoms** | | | |
| O1-H101 | 1.164(6) | Pt2-O1-H101 | 116.8(4) |
| O1-H201 | 0.834(6) | Pt2-O1-H201 | 119.2(5) |
| | | H101-O1-H201 | 113.9(6) |
| O3-H103 | 1.001(8) | H103-O3-H203 | 111.3(7) |
| O3-H203 | 1.233(8) | | |

[a] See footnote *a* of Table II. Distances have not been corrected for thermal motion.

**$[Pt_2(NH_3)_4(C_5H_4NO)_2(NO_3)_2](NO_3)_2 \cdot {}^1/_2H_2O$ (2).** The structure was solved and refined as described above for **1**. All non-hydrogen atoms were refined with anisotropic thermal parameters, and hydrogen atoms were refined with constraints using isotropic thermal parameters. The hydrogen atoms of each pyridonate ring and of the amine ligands N3 and N4 were each given an independent set of thermal parameters in the refinement. The hydrogen atoms of the N1 and N2 ammine ligands were refined with fixed thermal parameters ($U$ = 0.05 Å). The hydrogen atoms of the water molecule (O1), which lies on a crystallographic twofold symmetry axis, were not located. The nitrate group at N7 was disordered over two positions. The site occupancy factor (SOF) of each nitrate position (N7, O71, O72, O73, and N7, O74, O75, O76) was refined with the sum of the site occupation factors set equal to 1. The N7, O71, O72, O73 position was refined with independent positional and thermal parameters while that of N7, O73,

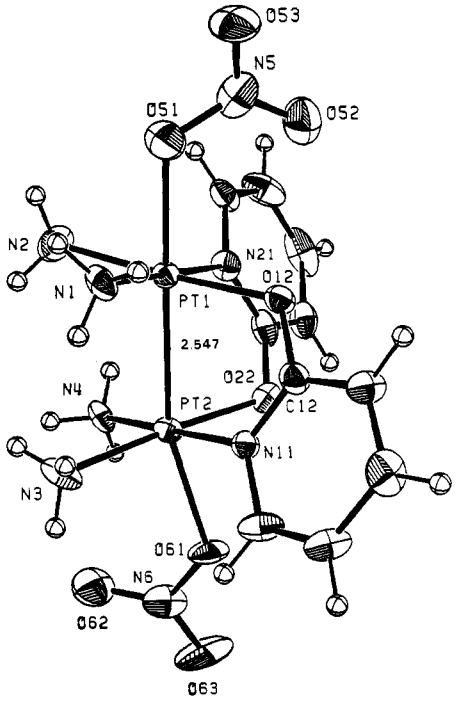


**Figure 3.** ORTEP illustration of the structure of the head-to-tail isomer of the α-pyridonate-bridged cation $[Pt_2(NH_3)_4(C_5H_4NO)_2(NO_3)_2]^{2+}$ (**2**), showing the 40% probability thermal ellipsoids and the Pt–Pt distance in angstroms. See caption to Figure 2.

O74, O75 was refined as a rigid group, with N7 as a pivot atom.[10]

Full-matrix least-squares refinement of the structure using 376 parameters converged at $R_1 = 0.036$ and $R_2 = 0.041$.[13] The weighting function used in the refinement was $w = 0.9585/[\sigma^2(F_o^2) + 0.000625F_o^2]$, and the maximum parameter shift in the final cycle of refinement was $0.2\sigma$ (O73 position). The only residual peaks of significant height (≤1.1 e Å$^{-3}$) that were observed in the final difference Fourier map were in the vicinity of N8 (<1.5 Å). The $w\Delta^2$ values for groups of data sectioned as above showed good consistency, and the weighting function was found to be acceptable.

The final atomic positional parameters with their estimated standard deviations are presented in Table III. The interatomic distances and angles with estimated standard deviations are reported in Table V. A complete listing of atomic positional and thermal parameters for compound **2** (Table S2) and a listing of observed and calculated structure factors (Table S4) are available as supplementary material. Figure 3 shows the coordination geometry and atom-labeling scheme for the $[Pt_2(NH_3)_4(C_5H_4NO)_2(NO_3)_2]^{2+}$ cation.

## Results and Discussion

**Description of the Structures. $[Pt_2(NH_3)_4(C_5H_4NO)_2(H_2O)(NO_3)][(NO_3)_3\cdot 2H_2O$ (1), Head-to-Head Dimer.** The binuclear cation (Figure 2) contains two *cis*-diammineplatinum(III) units bridged by two α-pyridonate ligands in a head-to-head arrangement. The Pt–Pt distance within the cation is 2.540 (1) Å, with both platinum atoms being six-coordinate. The two ligands that occupy the axial sites of the dimer are inequivalent. The platinum atom bound to the exocyclic pyridonate oxygen atoms (Pt2) contains a water molecule (O1) in the axial site while the platinum atom attached to the annular nitrogen atoms (Pt1) is coordinated to an oxygen atom (O51) of a nitrate anion. This result suggests that the exocyclic oxygen atoms of the two bridging α-pyridonate ligands provide more electron density to Pt2 than is provided to Pt1 by the ring nitrogen atoms. The latter platinum atom is therefore more electron deficient and binds the more negatively charged axial nitrate ligand. The axial and equatorial platinum–ligand distances are significantly different. While the Pt–O distances in the Pt2 equatorial plane compare favorably with Pt–O distances typically found in Pt(II) complexes (range 1.99–2.07 Å),[2,14] they are considerably shorter than the axial Pt–O distances. The Pt1–O51 distance (2.193 (7) Å) is ~0.18 Å longer than that found when nitrate is equatorially coordinated to platinum; for example, $Pt-O_{av}$ = 2.01 Å in *cis*-$[Pt(NH_3)_2(NO_3)_2]$.[15] A similar increase in the axial Pt2–O1 distance is revealed when this distance (2.122 (6) Å) is compared to the $Pt-OH_2$ distance of 2.052 (8) Å found in the mononuclear 1-methylcytosine complex *cis*-$[Pt(NH_3)_2(H_2O)(C_5H_7N_3O)](NO_3)_2\cdot H_2O$.[16] Elongated metal-to-axial ligand distances are observed in a large number of binuclear complexes containing metal–metal bonds[17] and are

Table V. Interatomic Distances (Å) and Angles (deg) for $[Pt_2(NH_3)_4(C_5H_4NO)_2(NO_3)_2](NO_3)_2\cdot{}^1/_2H_2O$ (**2**)[a]

| | | | |
|---|---|---|---|
| **Coordination Sphere** | | | |
| Pt1-Pt2 | 2.5468(8) | | |
| Pt1-N1 | 2.046(9) | Pt2-N3 | 2.058(9) |
| Pt1-N2 | 2.042(9) | Pt2-N4 | 2.057(9) |
| Pt1-N21 | 2.010(9) | Pt2-N11 | 2.024(9) |
| Pt1-O12 | 2.007(8) | Pt2-O22 | 1.991(8) |
| Pt1-O51 | 2.170(10) | Pt2-O61 | 2.165(10) |
| Pt2-Pt1-O51 | 176.3(3) | Pt1-Pt2-O61 | 163.9(3) |
| N1-Pt2-N2 | 90.1(4) | N3-Pt2-N4 | 90.9(4) |
| N1-Pt1-N21 | 178.6(4) | N4-Pt2-N11 | 177.4(4) |
| N1-Pt1-O12 | 89.1(4) | N4-Pt2-O22 | 88.3(3) |
| N2-Pt1-N21 | 90.4(4) | N3-Pt2-N11 | 91.3(4) |
| N2-Pt1-O12 | 176.5(4) | N3-Pt2-O22 | 176.1(4) |
| N21-Pt1-O12 | 90.4(4) | N11-Pt2-O22 | 89.5(4) |
| O51-Pt1-N1 | 79.8(4) | O61-Pt2-N4 | 92.6(4) |
| O51-Pt1-N2 | 83.2(4) | O61-Pt2-N3 | 92.9(4) |
| O51-Pt1-N21 | 99.0(4) | O61-Pt2-N11 | 85.9(4) |
| O51-Pt1-O12 | 93.3(4) | O61-Pt2-O22 | 83.3(3) |
| **Ligand Geometry** | | | |
| O12-C12 | 1.321(13) | O22-C22 | 1.334(15) |
| N11-C12 | 1.329(15) | N21-C22 | 1.320(17) |
| C12-C13 | 1.398(17) | C22-C23 | 1.404(17) |
| C13-C14 | 1.372(18) | C23-C24 | 1.388(20) |
| C14-C15 | 1.373(19) | C24-C25 | 1.363(22) |
| C15-C16 | 1.341(18) | C25-C26 | 1.347(19) |
| C16-N11 | 1.360(14) | C26-N21 | 1.359(14) |
| O12-N11 | 2.313(13) | O22-N21 | 2.299(16) |
| N5-O51 | 1.271(16) | N6-O61 | 1.279(15) |
| N5-O52 | 1.214(15) | N6-O62 | 1.218(16) |
| N5-O53 | 1.220(16) | N6-O63 | 1.213(16) |
| Pt2-N11-C12 | 118.7(7) | Pt1-N21-C22 | 120.2(8) |
| Pt2-N11-C16 | 122.7(9) | Pt1-N21-C26 | 120.6(9) |
| Pt1-O12-C12 | 119.2(7) | Pt2-O22-C22 | 117.6(8) |
| C12-N11-C16 | 117.9(10) | C22-N21-C26 | 119.2(11) |
| O12-C12-N11 | 121.6(11) | O22-C22-N21 | 120.0(11) |
| O12-C12-C13 | 117.3(11) | O22-C22-C23 | 118.7(13) |
| N11-C12-C13 | 121.2(11) | N21-C22-C23 | 121.3(12) |
| C12-C13-C14 | 119.2(12) | C22-C23-C24 | 117.8(14) |
| C13-C14-C15 | 119.2(12) | C23-C24-C25 | 120.1(14) |
| C14-C15-C16 | 118.8(12) | C24-C25-C26 | 119.0(14) |
| C15-C16-N11 | 118.3(8) | C25-C26-N21 | 122.6(14) |
| Pt1-O51-N5 | 122.6(10) | Pt2-O61-N6 | 125.8(10) |
| O51-N5-O52 | 121.0(16) | O61-N6-O62 | 118.8(15) |
| O51-N5-O53 | 116.8(13) | O61-N6-O63 | 116.4(16) |
| O52-N5-O53 | 122.2(15) | O62-N6-O63 | 124.7(16) |
| **Anion Geometry** | | | |
| N7-O71 | 1.215(12) | O71-N7-O72 | 120.7(13) |
| N7-O72 | 1.206(16) | O71-N7-O73 | 119.8(12) |
| N7-O73 | 1.210(18) | O72-N7-O73 | 117.7(14) |
| N7-O74[b] | 1.219 | O74-N7-O75 | 118.5 |
| N7-O75 | 1.216 | O74-N7-O76 | 118.4 |
| N7-O76 | 1.216 | O75-N7-O76 | 118.9 |
| N8-O81 | 1.222(16) | O81-N8-O82 | 118.7(15) |
| N8-O82 | 1.239(15) | O81-N8-O83 | 115.1(13) |
| N8-O83 | 1.172(16) | O82-N8-O83 | 124.7(16) |

[a] See footnote *a* of Table III. Distances have not been corrected for thermal motion. [b] Nitrate N7 is disordered over two positions; see footnote *b* of Table III.

(14) (a) Lock, C. J. L.; Peresie, H. J.; Rosenberg, B.; Turner, G. *J. Am. Chem. Soc.* **1978**, *100*, 3371. (b) Faggiani, R.; Lock, C. J. L.; Pollock, R. J.; Rosenberg, B.; Turner, G. *Inorg. Chem.* **1981**, *20*, 804. (c) Faggiani, R.; Lippert, B.; Lock, C. J. L.; Speranzini, R. A. *J. Am. Chem. Soc.* **1981**, *103*, 1111.
(15) Lippert, B.; Lock, C. J. L.; Rosenberg, B.; Zvaguli, M. *Inorg. Chem.* **1977**, *16*, 1525.
(16) Britten, J. F.; Lippert, B.; Lock, C. J. L.; Pilon, P. *Inorg. Chem.* **1982**, *21*, 1936.

a result of the structural trans influence of the metal–metal bond.[17,18] The Pt–N distances for both ammine and α-pyridonate nitrogen atoms are within the range normally found in related platinum(II) complexes (2.00–2.10 Å).[2,14] The Pt–$NH_3$ distances trans to the heterocyclic nitrogen atoms of the α-pyridonate ligands are an average of 0.017 Å longer than the Pt–$NH_3$ distances trans to the exocyclic oxygen atoms. This effect, which can also be attributed to the structural trans influence[18] where the donor strength of the heterocyclic nitrogen is greater than that of the amidate oxygen, is also found in the head-to-head and head-to-tail α-pyridonate-bridged platinum(II) complexes.[2]

Both platinum atoms in the α-pyridonate-bridged cation have similar coordination geometries. The angles between adjacent donor atoms within the equatorial planes of the platinum atoms are close to 90°. Two of the in-plane angles, N3–Pt2–N4 (93.2 (3)°) and N4–Pt2–O22 (85.6 (3)°) deviate significantly from 90°. Since the four equatorial ligands that are bound to Pt2 define a nearly perfect plane (rms deviation 0.0019 Å), the deviation of these two angles can be viewed as a ~3.3° tipping of N4 toward O22. Distortions of this magnitude also have been observed in other amidate-bridged platinum complexes[1c,2,14] and may result from hydrogen-bonding interactions in the lattice. The four equatorial ligands that are bound to Pt1 also lie in a plane (rms deviation 0.001 Å). Both platinum atoms are slightly displaced out of the equatorial plane toward one another (0.094 Å for Pt1 and 0.011 Å for Pt2). The tile angle ($\tau$) between the adjacent platinum coordination planes is 20.0°, and the average torsion angle (or twist) about the Pt–Pt bond ($\omega$) is 23.2°. The angles between adjacent equatorial and axial ligands are also close to 90°, with the angles about Pt2 showing the largest deviations (≤4.1°) from this value. As a result of the platinum–axial ligand bonds being nearly perpendicular to the equatorial platinum coordination planes, which are splayed by 20°, the Pt–Pt–axial ligand angles are less than 180° (Pt1–Pt2–O1 = 171.7 (2)° and Pt2–Pt1–O51 = 169.3 (2)°).

A comparison of the bond lengths and angles within the α-pyridonate ligands shows that both rings have equivalent geometries. The largest difference between the two rings is found in the N1–C2–C3 angle, which is 2.0° (1.8$\sigma$[19]) larger in ring 2. More significant differences are found in comparing the geometry of free α-pyridone[20] to that of the α-pyridonate ligands in compound **1**. As noted for the α-pyridonate-bridged complexes of platinum(II),[2] significant changes are observed in the bond lengths and angles at atoms (N1, C2, and O2) adjacent to the platinum binding sites. The internal ring angle C6–N1–C2 decreases from 123.5 (3)° in α-pyridone to 119.6(7)–119.7(8)° in compound **1** (a difference of 4.4$\sigma$), and the O2–C2–C3 angle decreases by ~7$\sigma$, from 125.9 (3)° to 118.6 (8)–119.3 (8)°. A similar increase in the adjacent internal ring angle N1–C2–C3 of 4.9° (~4$\sigma$) and in the N1–C2–O2 angle of 1.9° (2$\sigma$) occurs with platinum binding. Two bond lengths in the α-pyridonate ligands also differ significantly from those found in α-pyridone. The average C2–O2 distance is 0.043 Å (3.9$\sigma$) longer and the N1–C2 distance is 0.031 Å (2.8$\sigma$) shorter in the platinum complex. As a result of these changes in geometry, the ligand bite distance (N1–O2) is 0.028–0.034 Å (~3$\sigma$) longer in compound **1**.

The planarity of the α-pyridonate rings is maintained in the head-to-head dimer, with a rms deviation of the ligand atoms from the least-squares plane being 0.016 Å for ring 1 and 0.021 Å for ring 2. The platinum atoms lie out of these planes; the displacement from the ring 1 plane is 0.318 Å for Pt1 and 0.611 Å for Pt2 and from the ring 2 plane 0.218 and 0.743 Å, respectively. The dihedral angles between the platinum coordination planes and the planes of the α-pyridonate ligands are, for ring 1, 61.9° (Pt1 plane) and 77.4° (Pt2 plane) and, for ring 2, 74.2° (Pt1 plane) and 62.9° (Pt2 plane). The angles between the platinum atoms and pyridonate rings (Pt1–N1–C2, Pt1–N1–C6, and Pt2–O2–C2) are all close to 120°.

The geometry of the axial nitrate ligand (N5) is similar to that found in the platinum(II) complex *cis*-$[Pt(NH_3)_2(NO_3)_2]$.[15] One of the N–O bond lengths and one of the O–N–O bond angles are distorted relative to the geometry of free nitrate ion. The N–O bond to the oxygen atom (O51) that is coordinated to Pt1 is an average of 0.056 Å (4$\sigma$) longer than the other two normal N–O bond lengths, and the O51–N5–O52 angle is an average of 7° (5.6$\sigma$) smaller than the remaining two O–N–O bond angles. Nearly identical differences in the corresponding N–O bond length (~0.06 Å) and O–N–O bond angle (~6°) are found in the geometry of the oxygen-bound nitrate ligands in *cis*-$[Pt(NH_3)_2(NO_3)_2]$. The Pt1–O51–N5 angle in compound **1** is however 5.3° (4.5$\sigma$) larger than the corresponding angle in the bis(nitrato) complex. The orientation of the planar nitrate ligand (rms deviation 0.012 Å) is unique in compound **1** since it occupies an axial site. The plane of the nitrate N5 roughly bisects the N1–Pt1–N2 angle with a 40.0° dihedral angle between the $NO_3^-$ plane and the plane defined by atoms N1, Pt1, N21, O51. The nitrate plane is tilted toward the N1 ammine ligand which forms an intramolecular hydrogen bond with O53 (H1N1–O53 = 2.14 (3) Å, N1–H1N1–O53 = 139 (2)°). The remaining nitrate anions are also planar with a four-atom rms deviation of 0.004 Å for nitrate N6, 0.003 Å for nitrate N7, and 0.0001 Å for nitrate N8. The bond lengths and angles for each of these nitrate anions are normal.

The packing of compound **1** in the crystal lattice is achieved through extensive hydrogen bonding. The axial water molecule (O1) is hydrogen bonded to both a nitrate anion (N6) and a water molecule (O3). The plane of the water molecule makes a dihedral angle of 58.1° with the N3, Pt2, O22, O1 plane. The geometry of the water molecule O1 is similar to that of the axial water molecule in the dirhodium(II) tetrakis(carboxylato) complex $[Rh_2(O_2CCH_3)_4(H_2O)_2]$.[21] The hydrogen bond between O1 and the lattice water molecule (O3) is rather short, with an O1–O3 distance of 2.58 (1) Å, a H1O1–O3 distance of 1.512 (8) Å, and a O1–H101–O3 angle of 148.4 (4)°. Hydrogen bonds of this length are typically found in structures of carboxylic acids and generally are indicative of acidic hydrogen bond donors.[22] A packing diagram and further discussion of the hydrogen bonding and packing interactions may be found in ref 23.

The shortest nonbonded $NH_3\cdots NH_3$ contacts occur between adjacent platinum coordination planes (H2N1–H1N3 = 2.40 (7) Å and H3N1–H1N3 = 2.31 (8) Å) while the shortest contacts between ammine ligands in the same plane are between H2N2 and H2N4 (2.49 (6) Å) and between H3N2 and

(17) (a) Koh, Y. B.; Christoph, G. G. *Inorg. Chem.* **1979**, *18*, 1122, (b) Norman, J. G., Jr.; Renzoni, G. E.; Case, D. A. *J. Am. Chem. Soc.* **1979**, *101*, 5256, (c) Cotton, F. A.; Walton, R. A. "Multiple Bonds Between Metal Atoms"; Wiley: New York, 1982; Chapters 7 and 8 and references cited therein.
(18) Appleton, T. G.; Clark, H. C.; Manzer, L. E. *Coord. Chem. Rev.* **1973**, *10*, 335.
(19) The esd is calculated by using $\sigma = (\sigma_1^2 + \sigma_2^2)^{1/2}$, where $\sigma_1$ and $\sigma_2$ are the errors in the bond lengths or angles being compared.
(20) (a) Almlöf, J.; Kvick, Å.; Olovsson, I. *Acta Crystallogr., Sect. B* **1971**, *B27*, 1201. (b) Penfold, B. R. *Acta Crystallogr.* **1953**, *6*, 59.
(21) Cotton, F. A.; DeBoer, B. G.; La Prade, M. D.; Pipal, J. R.; Ucko, D. A. *J. Am. Chem. Soc.* **1970**, *92*, 2926; *Acta Crystallogr., Sect. B* **1971**, *B27*, 1664.
(22) Vinogradov, S. N.; Linnell, R. H. "Hydrogen Bonding"; Van Nostrand-Reinhold: New York, 1971; Chapter 7.
(23) Hollis, L. S. Ph.D. Dissertation, Columbia University, 1982.
(24) Matsumoto, K.; Fuwa, K. *J. Am. Chem. Soc.* **1982**, *104*, 897.
(25) Schagen, J. D.; Overbeek, A. R.; Schenk, H. *Inorg. Chem.* **1978**, *17*, 1938.
(26) Cotton, F. A.; Falvello, L. R.; Han, S. *Inorg. Chem.* **1982**, *21*, 2889.
(27) Cotton, F. A.; Falvello, L. R.; Han, S. *Inorg. Chem.* **1982**, *21*, 1709.

Table VI. Comparison of Geometric Properties of Related Platinum Complexes

| compd | formal Pt oxidn state | Pt–Pt dist, Å | dihedral angle, deg[a] τ | dihedral angle, deg[a] ω | ref |
|---|---|---|---|---|---|
| $[Pt_2(NH_3)_4(C_5H_4NO)_2(H_2O)(NO_3)](NO_3)_3\cdot 2H_2O$ (1) | 3.0 | 2.5401 (5) | 20.0 | 23.2 | *b* |
| $[Pt_2(NH_3)_4(C_5H_4NO)_2(NO_3)_2](NO_3)_2\cdot {}^1/_2H_2O$ (2) | 3.0 | 2.5468 (8) | 20.3 | 26.3 | *b* |
| $[Pt_2(NH_3)_4(C_5H_4NO)_2]_2(NO_3)_5\cdot H_2O$ (3) | 2.25 | 2.7745 (4)<br>2.8770 (9) | 27.4 | 22.8 | 1c |
| $[Pt_2(NH_3)_4(C_5H_4NO)_2]_2(NO_3)_4$ (4) | 2.0 | 2.8767 (7)<br>3.1294 (9) | 30.0 | 20.3 | 2 |
| $[Pt_2(NH_3)_4(C_5H_4NO)_2](NO_3)_2\cdot 2H_2O$ (5) | 2.0 | 2.8981 (5) | 28.8 | 13.0 | 2 |
| $[Pt_2(NH_3)_4(C_4H_6NO)_2]_2(NO_3)_6\cdot 3H_2O$ (6) | 2.5 | 2.702 (–)[c]<br>2.709 (–)[c] | 18.7 | *c* | 24 |
| $[Pt_2(CH_3)_4(C_2F_3O_2)_2(C_6H_7N)_2]$ (7) | 3.0 | 2.557 (1) | *c* | 22 | 25 |
| $K_2[Pt_2(SO_4)_4(OSMe_2)_2]\cdot 4H_2O$ (8) | 3.0 | 2.471 (1) | 0 | 0 | 26 |
| $Na_2[Pt_2(HPO_4)_4(H_2O)_2]$ (9) | 3.0 | 2.486 (2) | 0 | 0 | 27 |

[a] τ is the tilt angle between adjacent platinum coordination planes in the binuclear unit, and ω is the average torsion angle about the Pt–Pt vector. [b] This work. [c] Value not reported.

H1N4 (2.55 (7) Å). Steric interaction between the ammine ligands is minimized by twisting the coordination planes about the Pt1–Pt2 vector (ω = 23.2°).

**$[Pt_2(NH_3)_4(C_5H_4NO)_2(NO_3)_2](NO_3)_2\cdot {}^1/_2H_2O$ (2), Head-to-Tail Dimer.** The geometry of the head-to-tail α-pyridonate-bridged cation (Figure 3) is similar to that of the head-to-head isomer **1**. The Pt–Pt distance within the cation is 2.5468 (8) Å, and each platinum atom is six-coordinate. The axial site of both platinum atoms is occupied by an oxygen atom of a nitrate anion. In contrast to the case for the head-to-head complex, the primary coordination spheres of both Pt atoms in compound **2** are equivalent. The equatorial platinum–ligand distances are comparable to those in the head-to-head complex. The axial platinum–ligand distances of 2.170 (10) Å (Pt1–O51) and 2.165 (10) Å (Pt2–O61) are longer than the in-plane platinum–ligand distances, which range from 1.991 (8) to 2.058 (9) Å. The axial Pt–O distances are comparable (2σ) to the corresponding Pt–$ONO_2$ distance in compound **1**. The angles between adjacent ligands within the equatorial plane of the platinum atoms are close to 90°, with the largest deviation being 1.7° (N4–Pt2–O22 = 88.3 (3)°). The equatorial ligands of each Pt atom lie in a plane with a four-atom rms deviation of 0.019 Å for the Pt1 plane and 0.023 Å for the Pt2 plane. As observed in the head-to-head dimer **1**, the platinum atoms are slightly displaced out of the plane toward one another (0.042 Å for Pt1 and 0.023 Å for Pt2). The tilt angle between the two platinum coordination planes is 20.3°, and the average torsion angle about the Pt–Pt vector is 26.3°. Both of these values are similar to those found in the head-to-head complex.

The geometries of the α-pyridonate rings in the head-to-tail and head-to-head platinum(III) dimers are equivalent, with differences ≤3σ. In **2** the platinum atoms Pt1 and Pt2 are displaced out of the plane of ring 1 by 0.419 and 0.592 Å and out of the plane of ring 2 by 0.882 and 0.072 Å, respectively. The orientation of the α-pyridonate planes relative to the equatorial platinum coordination planes is also similar to that found in compound **1**. The dihedral angles between these planes are, for ring 1, 59.9° (Pt2 plane) and 75.3° (Pt1 plane) and, for ring 2, 77.3° (Pt2 plane) and 60.5° (Pt1 plane).

The axial nitrate ligands in the head-to-tail dimer assume different orientations relative to the platinum coordination planes. The orientation of the nitrate ligand N6 is similar to that observed in the head-to-head dimer with one of the oxygen atoms (O62) pointing between the two ammine ligands (N3, N4) of the platinum coordination plane. The geometry of this nitrate group is also quite similar to that found in compound **1**. The O61–N6 bond is longer (0.06 Å (av), 4.4σ) than the other two N–O bond lengths, and the O6–N6–O63 bond angle is an average of 5.3° (2σ) smaller than the other two O–N–O bond angles. The oxygen atom O62 forms an intermolecular hydrogen bond with the N4 ammine ligand (O62–H1N4 = 2.49 (8) Å, O62–H1N4–N4 = 143 (2)°). While the Pt2–O61 bond is nearly perpendicular to the Pt2 coordination plane, the O61 atom is tilted slightly toward the atoms N11, O22 (O61–Pt2–N11 = 85.9 (4)° and O61–Pt2–O22 = 83.3 (3)°). As a result, the Pt1–Pt2–O61 angle of 163.9 (3)° is 5.4° smaller than the corresponding angle in the head-to-head isomer.

The orientation of the nitrate ligand N5 is unique. The nitrate anion is rotated 154° about the Pt–Pt vector relative to nitrate group N6. While the ligand is tilted in a similar fashion relative to the Pt–O vector (Pt1–O51–N5 = 122.6 (10)°), the oxygen atom O52 points between the α-pyridonate rings and is not involved in an intramolecular hydrogen bond. The principal hydrogen bond contact to this nitrate ligand is from an ammine group (N4) of a neighboring cation (O53–H3N4 = 2.26 (5) Å, O53–H3N4–N4 = 148 (5)°). The bond lengths and angles within the nitrate ligand are similar to those found in the adjacent nitrate group (N6).

The ammine ligands of the divalent cation in **2** form a number of hydrogen bonds with the nitrate anions N7 and N8. The nitrate anion N7 is disordered over the two positions N7, O71, O72, O73 and N7, O74, O75, O76 with site occupation factors (SOF) for the positions of 0.747 and 0.253, respectively. The disorder involves two sets of oxygen positions and a common nitrogen position. The four atoms of each position define a plane with a rms deviation of 0.041 Å, and the dihedral angle between the planes is 29.9°. Details of the hydrogen-bonding interactions are given in ref 23, together with a packing diagram.

**Structural Comparison with Other Binuclear Platinum Complexes.** The structures of the α-pyridonate-bridged complexes of platinum(III) may be compared with the the analogous α-pyridonate-bridged complexes of platinum(II). A comparison of selected geometric features of these compounds is presented in Table VI. The head-to-head α-pyridonate-bridged platinum(III) dimer **1** contains a Pt–Pt single bond, and consequently the Pt–Pt distance in this complex is 0.337 Å shorter than the corresponding distance in the head-to-head platinum(II) tetramer (**4**), which does not contain a formal metal–metal bond. When the head-to-head platinum(II) complex is oxidized by removing one electron per tetranuclear unit, the mixed-valence complex *cis*-diammineplatinum α-pyridone blue (PPB) (**3**) is produced and the Pt–Pt distances are decreased by 0.102 Å (Pt1–Pt2) and 0.252 Å (Pt2–Pt2′, see Figure 1). The bridged Pt1–Pt2 distances in the head-to-head complexes show a continuous decrease as the metal oxidation state increases in the series Pt(II), Pt(2.25), Pt(III). While such an inverse relationship between the platinum–platinum distance and the platinum oxidation state has been used to calculate metal–metal bond order in one-dimensional

Table VII. Electrochemical Data[a]

| | CV | | | | | DPV | | | | CPC no. of electrons/ platinum |
|---|---|---|---|---|---|---|---|---|---|---|
| compd | $\Delta E_p$[b] | $E_p - E_{p/2}$[c] | $\Delta E_{1/2}$[d] | $E_{1/2}^1$ | $E_{1/2}^2$ | width[e] | $\Delta E_{1/2}$[d] | $E_{1/2}^1$ | $E_{1/2}^2$ | |
| 1 | 80 (10) | 52 (8) | 30 (10) | 0.63 (1) | 0.60 (1) | 110 (5) | 50 (10) | 0.65 (1) | 0.60 (1) | 0.90 |
| 2 | 48 (10) | 35 (4) | −30 (20) | 0.61 (1) | 0.64 (1) | 61 (5) | −15 (10) | 0.61 (1) | 0.63 (1) | 0.85 |
| 5 | 45 (10) | 35 (4) | −30 (20) | 0.61 (1) | 0.64 (1) | 60 (5) | −20 (10) | 0.61 (1) | 0.63 (1) | 0.95 |

[a] All reported potentials are in V vs. SCE. Numbers in parentheses denote the maximum range of values over several repeated experiments and thus are a measure of precision. [b] Peak-to-peak separation, $\Delta E_p = |E_p(\text{cathodic}) - E_p(\text{anodic})|$, in mV. [c] Width at $i_d/2$, in mV. [d] $E_{1/2}^1 - E_{1/2}^2$, in mV. [e] Full width at half $i_{max}$.

platinum complexes,[28] it is difficult to apply this empirical method to the discrete binuclear and tetranuclear complexes studied here. A number of factors such as axial ligand donor effects influence the metal–metal bond lengths in these compounds.[5] The platinum–platinum distances in the α-pyridonate-bridged complexes (**1–5**) and in the analogous head-to-head α-pyrrolidonate-bridged complex $[(NH_3)_2Pt(C_4H_6NO)_2Pt(NH_3)_2]_2(NO_3)_6 \cdot 3H_2O$ (**6**)[24] do, however, correlate with the calculated bond orders in a qualitative fashion. If the average platinum oxidation state is used to calculate an average bond order, the following descending series is obtained: Pt(III) dimers (**1**, **2**; bond order ~1) > Pt(2.5) tetramer (**6**; bond order ~1/3) > Pt(2.25) tetramer (**3**; bond order ~1/6) > Pt(II) dimers (**4**, **5**; bond order ~0). The Pt–Pt distances in this series increase as predicted on the basis of the estimated average bond order.

The cation geometry undergoes a number of changes in order to accommodate the range of Pt–Pt distances in the α-pyridonate-bridged complexes (**1–5**). The tilt angle ($\tau$) between the adjacent coordination planes decreases in a uniform fashion from 28.8–30.0° in the Pt(II) complexes (**4**, **5**) to 27.4° in PPB (**3**) to 20.0–20.3° in the Pt(III) complexes (**1**, **2**), as the bridged Pt–Pt distance decreases. The twist angle ($\omega$) of the platinum coordination planes about the Pt–Pt vector also increases in a uniform fashion as the Pt–Pt distance decreases. In the head-to-tail α-pyridonate-bridged complexes the twist angle increases from 13.0 to 26.3° as the Pt–Pt distance decreases from 2.898 Å in the Pt(II) dimer (**5**) to 2.547 Å in the Pt(III) dimer (**2**). The magnitude of the increase is smaller in the head-to-head complexes, where $\omega$ changes from 20.3 to 22.8 to 23.2°, as the Pt–Pt distance decreases from 2.877 Å in the Pt(II) dimer (**4**) to 2.775 Å in PPB (**3**) to 2.540 Å in the Pt(III) dimer (**1**). A similar twist angle of 22° is found in the structurally analogous trifluoroacetate-bridged platinum(III) dimer $[(Mepy)(CH_3)_2Pt(O_2CCF_3)_2Pt(CH_3)_2(Mepy)]$ (**7**; Mepy = 4-methylpyridine).[25] This complex contains a Pt–Pt single bond ($d$(Pt–Pt) = 2.557 (1) Å) between two *cis*-dimethylplatinum(III) units and elongated platinum-to-axial ligand bond lengths, Pt–N(Mepy) = 2.13 Å (av). The large twist angle in this complex and in the α-pyridonate-bridged platinum(III) complexes presumably is a result of the nonbonded repulsions between the in-plane ligands ($CH_3$ in **7** and $NH_3$ in **1** and **2**), which are minimized by the rotation of the planes about the Pt–Pt bond. The lack of this effect in the sulfate- (**8**) and phosphate-bridged (**9**) platinum(III) complexes, which contain parallel platinum coordination planes, may contribute to the shorter (~0.06 Å) Pt–Pt distances in these complexes (see Table VI).

The most significant differences in the geometry of the bridging framework of the Pt(II) and Pt(III) complexes are found in the angles made between the bonds involving the platinum and the α-pyridonate ring atoms. The platinum–platinum distances (~2.54 Å) in the platinum(III) complexes **1** and **2** are more closely matched by the α-pyridonate bite

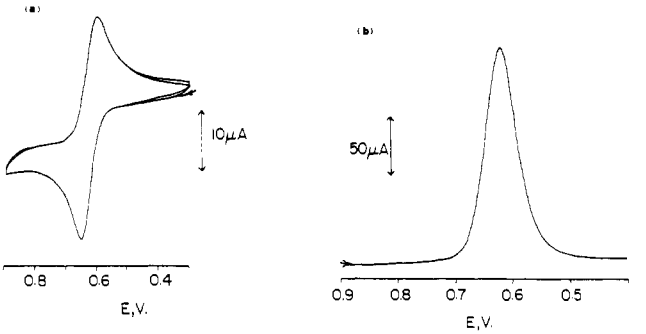


**Figure 4.** (a) Cyclic voltammogram for the head-to-tail platinum(II) dimer $[Pt_2(NH_3)_4(C_5H_4NO)_2](NO_3)_2 \cdot 2H_2O$ (**5**) (0.9 mM) showing several scans taken at a scan rate of 20 mV $s^{-1}$. (b) Differential pulse voltammogram for the head-to-tail platinum(III) dimer $[Pt_2(NH_3)_4(C_5H_4NO)_2(NO_3)_2](NO_3)_2 \cdot {}^1/_2H_2O$ (**2**) (0.4 mM).

distance (~2.30 Å) than are the longer distances (~2.90 Å) in the platinum(II) complexes **4** and **5**. Consequently, the angles between the platinum atoms and the α-pyridonate ring atoms are smaller in the Pt(III) complexes. In the head-to-tail Pt(III) dimer **2**, the Pt–N1–C2, Pt–N1–C6, and Pt–O2–C2 angles decrease by an average of 3.6 (4$\sigma$), 5.1 (5.7$\sigma$), and 8.8° (11$\sigma$), respectively, relative to the corresponding values in the head-to-tail Pt(II) dimer **5**. A similar decrease in the Pt–N1–C6 (3.8°, 3.9$\sigma$) and Pt–O2–C2 (6.2°, 6.6$\sigma$) angles is found in comparing the head-to-head Pt(III) complex **1** to the Pt(II) analogue **4**. The largest difference in the ring geometry is found in the N1–C2–O2 angle, which also decreases by an average of 2.9° (2.2$\sigma$) in the head-to-tail isomer and by 2.1° (2$\sigma$) in the head-to-head isomer, as the platinum distance decreases. The geometries of the in-plane ligands in both the Pt(II) and the Pt(III) complexes show no significant differences with the exception of the Pt–O2 bond lengths, which are slightly shorter in the Pt(III) complexes (0.028 Å, 2.8$\sigma$ in **1** and 0.025 Å, 2.4$\sigma$ in **2**), as expected from charge considerations.

**Electrochemical Studies.** The process of metal-metal bond formation in the head-to-tail and head-to-head α-pyridonate bridged dimers was examined by using cyclic voltammetry (CV), differential pulse voltammetry (DPV), and controlled-potential coulometry (CPC). The results of these studies are summarized in Table VII. Differential pulse and cyclic voltammetric techniques are frequently employed to determine the individual electrode potentials for multistep redox processes.[29,30] The shape of the voltammogram for a reversible two-step system is a function of the difference in the potential

(28) Reis, A. H., Jr.; Peterson, S. W. *Inorg. Chem.* **1976**, *15*, 3186.

(29) (a) Nicholson, R. S.; Shain, I. *Anal. Chem.* **1964**, *36*, 706, (b) Nicholson, R. S. *Ibid.* **1965**, *37*, 1351. (c) Polcyn, D.; Shain, I. *Ibid.* **1966**, *38*, 370, 376. (d) Myers, R. L.; Shain, I. *Ibid.* **1969**, *41*, 980. (e) Birke, R. L.; Kim, M.-H.; Strassfeld, M. *Ibid.* **1981**, *53*, 852.

(30) (a) Richardson, D. E.; Taube, H. *Inorg. Chem.* **1981**, *20*, 1278 and references cited therein. (b) Fenton, D. E.; Schroeder, R. R.; Lindvedt, R. L. *J. Am. Chem. Soc.* **1978**, *100*, 1931. (c) Fenton, D. E.; Lindvedt, R. L. *Ibid.* **1978**, *100*, 6367. (d) Louis, R.; Agnus, Y.; Weiss, R.; Gisselbrech, J. P.; Gross, M. *Nouv. J. Chim.* **1981**, *5*, 71.

of the individual one-electron steps ($\Delta E_{1/2} = E_{1/2}^1 - E_{1/2}^2$). For $\Delta E_{1/2}$ less than ~100 mV, the two individual waves are merged into one peak. Analysis of the CV peak parameters $E_p - E_{p/2}$ (peak width) and $\Delta E_p$ (peak-to-peak separation) and the DPV peak width ($\Delta E$ at $i_{max}/2$) can be used to determine $\Delta E_{1/2}$ for a two-step process.[29,30]

The electrochemical oxidation of the head-to-tail platinum(II) dimer **5** is found, from CV measurements, to approach reversibility at scan rates ($v$) in the 5–20 mV $s^{-1}$ range. A single wave is observed at $E_p$ = +0.63 V in the region examined, from +1.0 to −0.1 V (see Figure 4). The CV parameters ($\Delta E_p$ and $E_p - E_{p/2}$, Table VII) are consistent with a redox process that involves the exchange of 2 electrons/platinum dimer. This interpretation is confirmed by exhaustive electrolysis of the platinum(II) dimer at +0.85 V, which produces a colorless to orange color change in the solution and results in a net loss of 0.95 electron/platinum atom. CV and DPV experiments conducted after the electrolysis or on authentic samples of the resulting head-to-tail Pt(III) dimer **2** (Table VII) gave results identical, within precision error limits, with those observed prior to electrolysis. The CV parameters ($\Delta E_p$ and $E_p - E_{p/2}$), measured at scan rates where reversible behavior is observed (5–20 mV $s^{-1}$), also suggest the redox process involves the exchange of 2 electrons/platinum dimer. From the value of $E_p - E_{p/2}$, the potential difference ($\Delta E_{1/2} = E_{1/2}^1 - E_{1/2}^2$) for the two-step charge-transfer reaction (1)

$$Pt^{III}\text{–}Pt^{III} + e^- \overset{E_{1/2}^1}{\rightleftharpoons} Pt^{II}\text{–}Pt^{III} + e^- \overset{E_{1/2}^2}{\rightleftharpoons} Pt^{II}\text{–}Pt^{II} \qquad (1)$$

is estimated to be −30 mV.[29,30] This value is in good agreement with the value of −20 mV obtained for $\Delta E_{1/2}$ from the peak width in the DPV experiment (see Table VII). The negative value obtained for $\Delta E_{1/2}$ indicates that the removal of the second electron from the platinum(II) dimer is assisted by the removal of the first. The magnitude of $\Delta E_{1/2}$ should be viewed as an approximation, however, since, as discussed below, the electron transfer is coupled to a chemical reaction.

Concerted two-electron charge-transfer reactions are uncommon in binuclear transition-metal complexes.[30] Several binuclear copper complexes[30b-d] undergo concerted two-step charge-transfer reactions, but these redox processes do not involve metal–metal bond formation. As observed in the case of the tetrakis(μ-carboxylato)dirhodium(II) complexes, $Rh_2(O_2CR)_4$,[31] most redox reactions involving metal–metal bond formation in binuclear complexes proceed through sequential one-electron steps.[32,33]

The cyclic voltammetric behavior of the head-to-tail platinum(II) dimer as a function of scan rate is shown in Figure 5. At scan rates greater than 20 mV $s^{-1}$ both $\Delta E_p$ and the ratio of the anodic to cathodic peak currents ($i_a/i_c$) increase and $i_a v^{-1/2}$ decreases as $v$ increases. This behavior indicates that the oxidation of the Pt(II) complex is coupled to a chemical reaction, as expected from the fact that two axial ligands ($H_2O$ and/or $NO_3^-$), not present in the starting binuclear Pt(II) complex, are coordinated in the resulting Pt(III) dimer. Since the axial ligands of the head-to-tail Pt(III) dimer are exchangable in an aqueous medium,[5,34] the rate of the ligand-exchange reactions could well be affecting the electrochemical parameters at the faster scan speeds. At present we have no kinetic information as to when, during the electrochemical process, the chemical reactions occur.

The electrochemical behavior of the head-to-head platinum(III) dimer **1** is similar in some respects to that observed for the head-to-tail α-pyridonate-bridged complex **2**. A single wave is observed at $E_p$ = +0.63 V in both CV and DPV measurements. From the dependence of the CV peak parameters ($\Delta E_p$, $i_a/i_c$, and $i_a v^{-1/2}$) on the voltage scan rate, the redox process also appears to be coupled to a chemical reaction. CPC measurements show that two electrons are transferred per platinum dimer during the reduction. The major difference between the electrochemical behavior of the head-to-head and head-to-tail dimers is the kinetics of the coupled chemical reactions. In the case of the head-to-head complex, the CV parameters $\Delta E_p$, $i_a/i_c$, and $i_a v^{-1/2}$ vary as a function of $v$ down to the slowest measured scan rate (5 mV $s^{-1}$) and never become constant. From the controlled-potential electrolysis experiments, it is evident that a chemical reaction in addition to axial ligand exchange accompanies the electron transfer. As the reductive electrolysis of compound **1** proceeds to completion, the solution changes color from orange to green to blue and finally becomes colorless. The blue color that is produced during the reduction is most intense after a total of 1.5 electrons are added per platinum(III) dimer. These results suggest that the reduced platinum complex reacts with the platinum(III) dimer to produce the tetranuclear mixed-valent platinum blue (PPB) following the electron transfer. With the assumption that the redox process approaches the reversible behavior in the slow scan rate limit, the CV and DPV parameters can be used to estimate $\Delta E_{1/2}$ of the two-step charge transfer. With this approximation, the value of $\Delta E_{1/2}$ lies in the range of +30 to +50 mV (Table VII). The positive value of $\Delta E_{1/2}$ implies that the charge transfer occurs in two one-electron steps. These results are consistent with the appearance of PPB, which is the product of a one-electron oxidation, during the controlled-potential electrolysis experiments. Since the value of $\Delta E_{1/2}$ suggests that the mixed-valent Pt(II)–Pt-

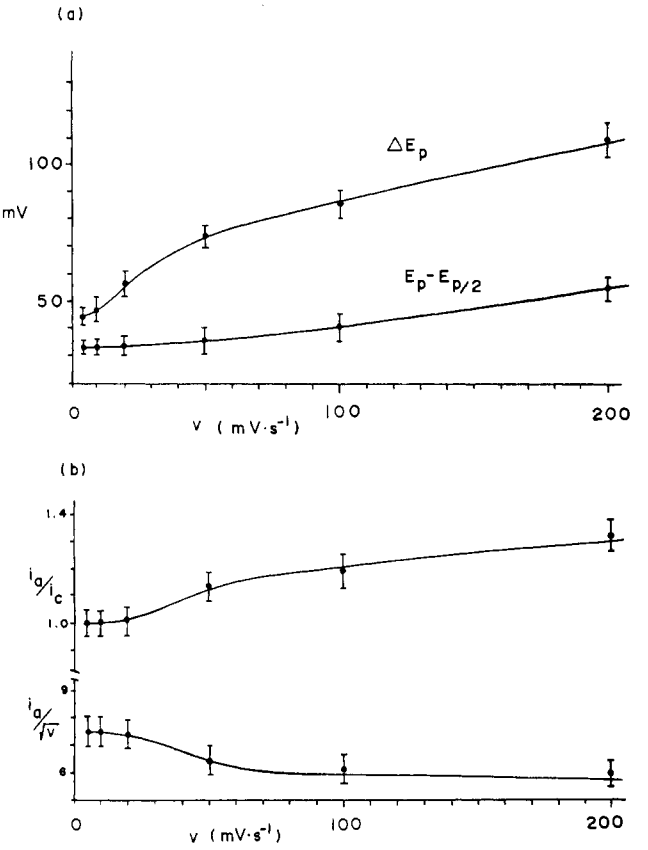


**Figure 5.** (a) Variation of the CV parameters $\Delta E_p$ and $E_p - E_{p/2}$ as a function of scan rate ($v$) for the head-to-tail platinum(II) dimer **5**. (b) Ratio of the anodic to cathodic peak currents ($i_a/i_c$) and the anodic peak current to the square root of the voltage scan rate ($i_a/v^{1/2}$) for compound **5**. The horizontal bars represent the observed variation of the measurement.

(31) Das, K.; Kadish, K. M.; Bear, J. L. *Inorg. Chem.* **1978**, *17*, 930.
(32) Reference 17c, pp 62–64, 187–190 and references cited therein.
(33) Kadish, K. M.; Lancon, D.; Dennis, A. M.; Bear, J. L. *Inorg. Chem.* **1982**, *21*, 2987.
(34) Hollis, L. S.; Lippard, S. J., unpublished results.

(III) dimer is produced during the reduction of the Pt(III) head-to-head dimer, the reactions (2) and (3) are probably involved in the electrochemical generation of PPB.

$$Pt^{III}\text{–}Pt^{III} + e^- \overset{E_{1/2}^1}{\rightleftharpoons} Pt^{II}\text{–}Pt^{III} + e^- \overset{E_{1/2}^2}{\rightleftharpoons} Pt^{II}\text{–}Pt^{II} \quad (2)$$

$$Pt^{II}\text{–}Pt^{III} + Pt^{II}\text{–}Pt^{II} \rightleftharpoons Pt^{II}\text{–}Pt^{III}\text{–}Pt^{II}\text{–}Pt^{II}\ (PPB) \quad (3)$$

In the multistep charge-transfer reactions of this type, self-exchange reactions must also be considered:[30a]

$$Pt^{II}\text{–}Pt^{II} + Pt^{III}\text{–}Pt^{III} \overset{K_c}{\rightleftharpoons} 2Pt^{II}\text{–}Pt^{III} \quad (4)$$

The estimated value of $\Delta E_{1/2}$ can be used to calculate the comproportionation constant ($K_c$) for the system at equilibrium. The equilibrium constant can be estimated[30a] by using the relationship (5). If it is assumed that the difference in

$$K_c = \frac{[Pt^{II}\text{–}Pt^{III}]^2}{[Pt^{II}\text{–}Pt^{II}][Pt^{III}\text{–}Pt^{III}]} = \exp(n_1 n_2 F \Delta E^\circ / RT) \quad (5)$$

the standard reduction potentials ($\Delta E^\circ$) for the two-step process is $\sim \Delta E_{1/2}$, the calculated value for $K_c$ is in the range $3 < K_c < 7$. This approximate value for $K_c$ suggests that the formation of the mixed-valent $Pt^{II}$–$Pt^{III}$ species is thermodynamically favorable. Although further studies on the kinetics of these reactions will be required to determine the importance of the $Pt^{II}$–$Pt^{III}$ complex in the formation of PPB, it is noteworthy that a $(Pt^{II}\text{–}Pt^{III})_2$ compound has been obtained from the reactions of *cis*-diammineplatinum(II) with α-pyrrolidone, compound **6**.[24]

Quasi-reversible behavior is observed in the CV studies of pure samples of PPB, and exhaustive electrolysis at +0.80 V results in a net loss of 0.67 electron/platinum atom. These experiments also suggest that the Pt(III) head-to-head dimer is produced upon oxidative electrolysis. A similar result was found in earlier potentiometric studies of PPB. Two independent reports[1e,35] on $Ce^{IV}$ titrations of PPB suggested that Pt(III) species were produced during the redox titrations. The results presented here confirm these earlier observations.

## Conclusion

Structural and electrochemical studies show that metal–metal-bonded Pt(III) dimers can be prepared from the oxidation of both the head-to-tail α-pyridonate-bridged platinum(II) dimer (**5**) and *cis*-diammineplatinum α-pyridone blue (PPB). Electrochemical studies show that metal–metal bond formation in the head-to-tail dimer proceeds through a concerted two-electron charge-transfer process which is coupled to a chemical reaction. In the head-to-head dimer, the metal–metal bond in the platinum(III) complex appears to form through two one-electron steps which are also coupled to a chemical reaction. In this case the coupled chemical reaction may involve the formation of PPB through a multistep process.

**Acknowledgment.** This work was supported by National Institutes of Health Research Grant CA-15826. We thank Engelhard Industries for a loan of $K_2PtCl_4$ used to make all platinum complexes.

**Registry No.** **1**, 86308-22-7; **2**, 86362-05-2; **3**, 62782-86-9; **5**, 76775-76-3.

**Supplementary Material Available:** Listings of atomic positional and thermal parameters for compounds **1** and **2** (Tables S1 and S2) as well as final observed and calculated structure factors (Tables S3 and S4) (33 pages). Ordering information is given on any current masthead page.

(35) Laurent, M. P.; Tewksbury, J. C.; Krogh-Jespersen, M.-B.; Patterson, H. *Inorg. Chem.* **1980**, *19*, 1656.

---

Contribution from the Department of Chemistry, Simon Fraser University, Burnaby, British Columbia, Canada V5A 1S6

# Bimetallic Aryldiazenido Complexes. Crystal and Molecular Structure of $(\eta^5\text{-}C_5H_5)(CO)_2Mo(\mu\text{-}NNC_6H_4CH_3)Re(CO)_2(\eta^5\text{-}C_5H_5)$ Possessing a $\mu$-Aryldiazenido-*N*,*N*′ Bridge

CARLOS F. BARRIENTOS-PENNA, FREDERICK W. B. EINSTEIN, TERRY JONES, and DEREK SUTTON*

*Received November 30, 1982*

The title compound has been synthesized from the reaction of $CpMo(CO)_2(p\text{-}N_2C_6H_4CH_3)$ (Cp = $\eta^5$-$C_5H_5$) with $CpRe(CO)_2(THF)$ (THF = tetrahydrofuran) and its structure determined by X-ray crystallography. It crystallizes in space group $P\bar{1}$ with $a$ = 11.201 (3) Å, $b$ = 10.117 (3) Å, $c$ = 12.282 (4) Å, $\alpha$ = 115.34 (3)°, $\beta$ = 118.11 (2)°, $\gamma$ = 94.34 (3)°, and $Z$ = 2. The calculated and measured densities are 2.055 and 2.08 (1) g cm$^{-3}$, respectively. On the basis of 2525 observed X-ray-counter-measured intensities with $I \geq 2.3\sigma(I)$ in the range $45° \geq 2\theta$ (Mo K$\alpha$), the structure was solved and refined by full-matrix least-squares methods to $R$ = 0.024 and $R_w$ = 0.033. The bimetallic complex may be described as a $Cp(CO)_2Mo(NNC_6H_4CH_3)$ molecule coordinated through the exo nitrogen atom (N′) of its singly bent aryldiazenido ligand to a $CpRe(CO)_2$ fragment. The MoNN′ skeleton remains essentially linear. Important dimensions are Mo–N(2) = 1.822 (4) Å, Re–N(1) = 2.152 (4) Å, N(1)–N(2) = 1.256 (6) Å, Mo–N(2)–N(1) = 177.7 (4)°, and Re–N(1)–N(2) = 118.9 (3)°.

## Introduction

In mononuclear complexes, organodiazenido ligands ($N_2R$) (R = alkyl or aryl) have been found to exhibit two common structural types: the "singly bent" structure (A) where $N_2R$ is formally a 3-electron donor and the "doubly bent" structure (B) where $N_2R$ is formally a 1-electron donor.

With these as a basis, a number of potential structures for bimetallic organodiazenido complexes can be visualized, such as C–E. Structure D has been found to occur in the aryldiazenido complexes $Mn_2(CO)_8(N_2Ph)_2$,[1] $HOs_3(CO)_{10}(p$-

(1) Churchill, M. R.; Lin, K.-K. G. *Inorg. Chem.* **1975**, *14*, 1133.

0020-1669/83/1322-2614$01.50/0 